RSC Advances

PAPER

Cite this: *RSC Adv.*, 2015, **5**, 47022

# Modelling the effects of surfactant loading level on the sorption of organic contaminants on organoclays†

Qing Zhou,[abc] Runliang Zhu,*[ab] Stephen C. Parker,*[d] Jianxi Zhu,[ab] Hongping He[ab] and Marco Molinari[d]

Organoclays can effectively uptake organic contaminants (OCs) from water media, but the sorption mechanisms are not fully established yet, because of the lack of recognition of interlayer structure of organoclays. To unravel this complex behavior, we have examined the effects of surfactant loading on the interlayer structure and sorption behaviors of organoclays using molecular dynamics (MD) simulations. The sorption behavior of phenol on three cetyltrimethylammonium intercalated montmorillonite (CTMA-Mt) with CTMA loading levels of 0.33, 1.0, and 1.66 times of the Mt's cation exchange capacity (CEC), was studied. The results demonstrated that CTMA aggregates were the main sorption domains for phenol molecules, consistent with a partition process. The interlayer structure of CTMA-Mt influences the sorption affinity of phenol. CTMA aggregates increased in size with increasing loading level, creating larger sorption domains for phenol uptake. On the other hand, high CTMA loading level decreased the sorption affinity of CTMA-Mt (with 1.66 CEC loading) toward phenol by increasing the packing density and cohesive characteristic of the aggregates. In addition, the siloxane surfaces of Mt and the hydrated inorganic ions ($Ca^{2+}$ or $Br^{-}$) showed specific interactions with phenol molecules by forming H-bond. The oxygen atoms on siloxane surface and water molecules around $Br^{-}$ serve as H-bond acceptor while water molecules around $Ca^{2+}$ serve as H-bond donor, corresponding to polyparameter linear free energy relationships (pp-LFERs) results. The modelling results correlate well with the experimental findings, and further reveal that the sorption affinity strongly depends on the size and packing density of surfactant aggregates. In addition, H-bond interactions should be considered as well in the sorption of OCs containing particular groups.

Received 4th April 2015
Accepted 21st May 2015

DOI: 10.1039/c5ra05998d

www.rsc.org/advances

## Introduction

Organoclays are synthesized by exchanging the interlayer inorganic cations using cationic surfactants (*e.g.* cetyltrimethylammonium (CTMA)), to effectively and efficiently uptake organic contaminants (OCs) from aqueous media.[1–9] However, the sorption mechanisms underlying the uptake process have not been unambiguously clarified yet. Early studies indicated that the sorption of OCs was primarily a partition process, *i.e.*, partition of OCs between bulk water and the organic phases formed by surfactant aggregates in organoclays.[3–6] More recent studies, however, have shown that the sorption mechanism is not just a simple partition process as the organic carbon-normalized sorption coefficient ($K_{oc}$) of a given OC varies over one order of magnitude on different organoclays.[6–18] Thus, the sorption results from the change in the microstructure of the organoclays, which depends on an intricate play between different depending on factors such as charge type and density of clay minerals,[8–14] molecular structure and loading level of cationic surfactants.[5,6,13–21]

Of particular interest is the effect of surfactant loading on $K_{oc}$. $K_{oc}$ for a given OC often shows an evolution trend that first increases and then decreases with increasing surfactant loading level, with the maximum value generally appearing at ~1.0 times of the cation exchange capacity (CEC) of the clay minerals.[13–19,22] To explain this curious change in sorption behavior various hypothesis have been proposed. Bonczek *et al.*[22] proposed that organoclays with larger basal spacing have greater interlayer accessibility for OCs, while Chen *et al.*[16] suggested that the intercalated cationic surfactant forms adsorptive films with high affinity toward OCs at relatively low loading level and bulk organic phases with weak affinity toward OCs at high loading

[a]*Key Laboratory of Mineralogy and Metallogeny, Guangzhou Institute of Geochemistry, Chinese Academy of Sciences, Guangzhou 510640, China. E-mail: zhurl@gig.ac.cn; Fax: +86-020-85297603; Tel: +86-020-85297603*

[b]*Guangdong Provincial Key Laboratory of Mineral Physics and Material Research & Development, Guangzhou 510640, China*

[c]*University of Chinese Academy of Sciences, Beijing 100049, China*

[d]*Department of Chemistry, University of Bath, Claverton Down, Bath BA2 7AY, UK. E-mail: S.C.Parker@bath.ac.uk; Fax: +44 (0)1225-386231; Tel: +44 (0)1225-386505*

† Electronic supplementary information (ESI) available. See DOI: 10.1039/c5ra05998d

level. Bartelt-Hunt *et al.*[18] and Zhu *et al.*[13,14] proposed a change in the microstructure of the surfactant aggregates at different loading level, which leads to a different sorption affinity toward OCs, while Xu *et al.*[19] and Bonczek *et al.*[22] suggested that the hydration of interlayer inorganic ions decreases the hydrophobicity of the interlayer space, which leads to a decrease of $K_{oc}$. These wide range of explanations can be attributed to the structure of the interlayer, which is rather complex (*e.g.* arrangement of intercalated surfactant, solvent molecules, and intercalated ions) and can hardly be characterized by experimental techniques, particularly in an aqueous environment.

Molecular modelling is an efficient method for understanding the interlayer structure of clay minerals and organoclays by giving atom-level insights into structural features and transport properties.[23–29] Zhao and Burns[32,33] and Zhu *et al.*[30] showed that OCs molecules were primarily sorbed within CTMA aggregates. Shapley *et al.*[34] calculated a negative free energy for the sorption of polychlorinated dibenzo-*p*-dioxins (PCDDs) from bulk water into the interlayer space of CTMA montmorillonite (CTMA-Mt), finding that intercalated CTMA creates a hydrophobic environment for the sorption of PCDDs. These molecular modelling studies further proved the sorption of OCs on organoclays is primarily a partition process.

Although, the modelling research has laid the foundations to understand the atom-level interaction between OCs and CTMA-Mt, the experimental observations are still not fully understood and the effect of surfactant loading on the sorption of OCs remains unexplained. Thus, this work explores the effects of surfactant loading on the interlayer structure and sorption behaviors of organoclay CTMA-Mt using MD simulations, to provide fundamental understanding of the experimental findings and in general on the sorption mechanisms of OCs in organoclays.

# Materials and methods

## 1. Models

Mt model with chemical formula $Ca_{0.375}[Al_{3.25}Mg_{0.75}][Si_8]\cdot O_{20}(OH)_4$ was used as in previous studies.[28] In this model, the isomorphic substitutions obey Loewenstein's rule.[35] The simulation cell has dimensions of 20.80 Å × 36.02 Å × variable Å, comprising of two layers of 16 unit cells of montmorillonite ($4x \times 4y \times 1z$ expansion). The surfactant cetyltrimethylammonium (CTMA) was chosen to allow for comparison with previous studies.[13,17,28,30] 4, 12, 20 CTMA ions, representing three loading levels of CTMA, *i.e.*, 0.33, 1.00, and 1.66 times of Mt's CEC, were intercalated into the Mt interlayer to study the effect of the loading on the structure of the interlayer. For 0.33 CTMA loading, 4 $Ca^{2+}$ ions were added to the interlayer, while for 1.66 CTMA loading, 8 $Br^-$ ions were added to maintain overall charge neutrality of the simulation cell. To model the water saturated conditions, water molecules were gradually added (50 molecules at each step) into the interlayer of CTMA-Mt, until the basal spacing value was close to experimental $d_{001}$ values of wet samples (28.2 Å for 0.33 CTMA loading, 30.5 Å for 1.00 CTMA loading, 36.5 Å for 1.66 CTMA loading).[28,30] Finally, the water amount for 0.33, 1.0 and 1.66 CTMA loading was 400, 300, 300 respectively. Phenol was selected as representative of OCs as it has both nonspecific van der Waals interaction and specific H-bond interaction with CTMA-Mt and water.[30] Experiments showed that the adsorption amount of phenol is about 12.3 mg $g^{-1}$ of sorbed concentration, corresponding to 4.24 phenol molecules in our simulation system.[30] In addition, adsorption of phenol did not cause the increase of basal spacing of CTMA-Mt, indicating that some of the water molecules left the interlayer space during the sorption process. To clarify the exact number of water molecules replaced by phenol, a serious of test modelling have been performed by increasing the water/phenol ratio from 3 to 6. The results showed that when 4 water were replaced by 1 phenol, the basal spacing values remained constant.[30] Therefore, the sorption of phenol into water saturated CTMA-Mt was modeled by adding 4 phenol molecules randomly into the interlayer while 16 water molecules were removed.

## 2. Molecular modelling methods

MD simulations were undertaken using the DL_POLY code (version 2.20).[36] Classical potential modelling based on the Born model description of the ionic lattice assumes the interaction forces between ions consist of a long-range Coulombic term and a short-range potential. The equations of motion were updated using the Verlet–Leapfrog algorithm and the Ewald method was used for evaluating the electrostatic interactions. A short range potential cutoff of 9.5 Å was used and three dimensional periodic boundary conditions were applied.

CLAYFF force field was applied to simulate the system.[37] CLAYFF has been widely and successfully used for modelling clay minerals and organoclays.[23–34] In this force field, the interactions between the atomic species are described by Lennard-Jones parameters and Coulombic terms with partial charge, while hydroxyl groups (OH) are described by a harmonic term. The water solvent was represented by using the single point charge (SPC) water model as implemented within CLAYFF.[37,38] The CVFF force field was used to represent CTMA and phenol.[39] CVFF has been successfully used in the simulations of mineral–organic interfaces and alkylammonium intercalated Mt.[28–30] The strength of this combination of force field is that all use Lennard-Jones parameters and partial charges that can be mixed by using simple mixing rules.[37]

We applied a geometry optimization to each simulation cell first to obtain the minimum energy structure, which ensured a faster equilibration. Then, NPT (300 K, 1 atm) simulations were performed for 3 ns to achieve equilibrium, and another 1 ns to record the basal spacings. When systems reach equilibrium, the volume was fixed and a further 3 ns NVT (300 K) simulations and data collection were performed. In all simulations the time step was set to 1.0 fs and all atoms were allowed to move.

Through post-analysis of the MD trajectories, 2D-density profiles, *Z*-densities, radial distribution function (RDF), average H-bond number, self-diffusion coefficients and occupied volume of CTMA cations were analyzed as previously described.[34,40,41] The 2D-density profile is the 2 dimensional time-averaged (over the duration of the simulation) density

plots which give qualitative information not only about how dense the CTMA and phenol in the interlayer but also the favored adsorption sites. The *Z*-density was calculated dividing the system into slices of 0.3 Å along the *z* direction. The H-bond between phenol and water molecules was determined by imposing two conditions: (1) a distance between the donor and accepter smaller than 3 Å; (2) a H–O···O angle smaller than 30°.[42] The packing density was evaluated from the mass divided by the occupied volume of CTMA cations. The occupied volume of CTMA cations was calculated by subtracting the occupied volume of other interlayer species (including water, phenol, $Ca^{2+}$ and $Br^{-}$) from the interlayer spaces, and then the packing densities of CTMA aggregates was further calculated. The height of the interlayer space was determined considering the van der Waals radius of siloxane surface. Though the density of water varies with different interlayer spacing because of the confining effect of Mt layer, previous simulations have shown that the change of water density in the interlayer of water saturated CTMA-Mt with increasing loading level is negligible and the density mainly based on the chosen water potential model.[28] So the volume of single water molecule was 0.0297 $nm^3$ basing on the SPC water model.[38] Phenol was calculated to be 0.1458 $nm^3$ basing on a NPT ensemble simulation of 1500 water and 4 phenol under same *P*–*T* conditions. The volume of $Ca^{2+}$ and $Br^{-}$ was 0.0042 $nm^3$ and 0.0315 $nm^3$ basing on their ion radii.

## Results and discussion

### 1. Arrangement of the interlayer species

The snapshots, 2D density profiles of CTMA carbon on the alkyl chain (C3) and phenol carbon (CR), and *Z*-density profiles of the interlayer species of 0.33 CTMA-Mt, 1.0 CTMA-Mt, and 1.66 CTMA-Mt were compared (Fig. 1). The results showed that the charged head groups of CTMA cations were directly attached to the siloxane surface, although the head groups are not tethered to the surface, which could be attributed to the electrostatic interactions between the positively-charged head groups and the negatively charged siloxane surface.[28,30] The alkyl chains tended to either adsorb onto the siloxane surface or extend into the interlayer space forming alkyl chain aggregates. The loading level of CTMA affected the size of the CTMA aggregates. At low loading level (*i.e.*, 0.33 CTMA-Mt), a large portion of the alkyl chains adsorbed onto the siloxane surface while only a small amount extended into the interlayer space to form aggregates (Fig. 1a). With increasing CTMA loading level, more alkyl chains extended in the interlayer space to form aggregates, and accordingly the size of CTMA aggregates increased. In 1.66 CTMA-Mt, the CTMA loading exceeded the cation exchange capacity of Mt, causing $Br^{-}$ enter the interlayer space as counter ions. Some bromine ions resulted trapped into the aggregates. This caused the head groups of the extra CTMA (together with interlayer water molecules) to re-locate in the middle of the interlayer space, while their alkyl chains stretched away to form aggregates with CTMA cations (Fig. 1c). This is again related to the electrostatic interaction within to oppositely charged groups.

The transport properties of CTMA were investigated by calculating the self-diffusion coefficients of C3 (CTMA carbon on the alkyl chain). It was found that $D_{C3}$ decreased with CTMA loading level (Table 1). The low mobility of CTMA at its high loading level arises from the high packing density. Although several experimental studies suggested that the packing density of CTMA should increase with loading level, this work for the first time accurately calculated the packing density of CTMA aggregates on water-saturated CTMA-Mt, which was shown to increase with increasing loading level (Table 1). Thus, this work clearly shows that the packing density of CTMA increased with its loading level, indicating indeed that the interlayer microstructure changes radically depending on the CTMA loading level.

When phenol was present in the interlayer, it was mainly located within the CTMA aggregates on 1.0 CTMA-Mt and 1.66 CTMA-Mt (Fig. 1b and c), which suggested a partition mechanism for uptaking phenol, consistent with previous experimental and modelling results.[9–15,30–34] On the other hand, as the size of CTMA aggregate on 0.33 CTMA-Mt was rather small, some of the phenol molecules were sorbed on the surface of the CTMA aggregate (Fig. 1a). This indicates that at low CTMA loading level, the surfactant was unable to form large aggregates which are likely responsible for phenol uptake. The transport properties of phenol were also investigated by calculating the self-diffusion coefficients of CR (phenol carbon) (Table 1). Phenol showed higher mobility in 0.33 CTMA-Mt, but similar lower mobility in 1.0 CTMA-Mt and 1.66 CTMA-Mt, indicating the confining effect from CTMA aggregates, in accordance with 2D density profile (Fig. 1). Thus, we infer that as the structure of the nano-sized surfactant aggregates changes with surfactant loading level, their interactions with OCs will be affected to a different extent. Besides the organic cations, the siloxane surface also contribute to the sorption of phenol molecules. Phenol indeed could be sorbed on the siloxane surface through the –OH group as the oxygen atoms of the siloxane surface could act as H-bond acceptor.[30]

Although the arrangement of interlayer cations in montmorillonite has been reported by previous studies, the distribution of interlayer cations and anions in water saturated organoclays was not well discussed. Our modelling results showed that $Ca^{2+}$ cations on 0.33 CTMA-Mt mainly located close to the siloxane surface (Fig. 1a), which is attributed to the electrostatic interactions between them. According to the snapshot and *Z*-density profiles, $Ca^{2+}$ cations resided on the siloxane surface, similarly to previous modelling study on montmorillonite without intercalated organic cations.[27] From the RDF profiles of Ca-OW (water oxygen) and Ca-HC (CTMA hydrogen), the coordination number of water molecules surrounding $Ca^{2+}$ cations was calculated to be 7–8 water molecules, indicating that there is no direct interaction between $Ca^{2+}$ and CTMA molecules (Fig. 2a). On the other hand, $Br^{-}$ anions on 1.66 CTMA-Mt, almost completely located in the middle of interlayer space, *i.e.*, away from the siloxane surface (Fig. 1c), which is attributed to the electrostatic interaction between $Br^{-}$ and the head group of CTMA, and the

 

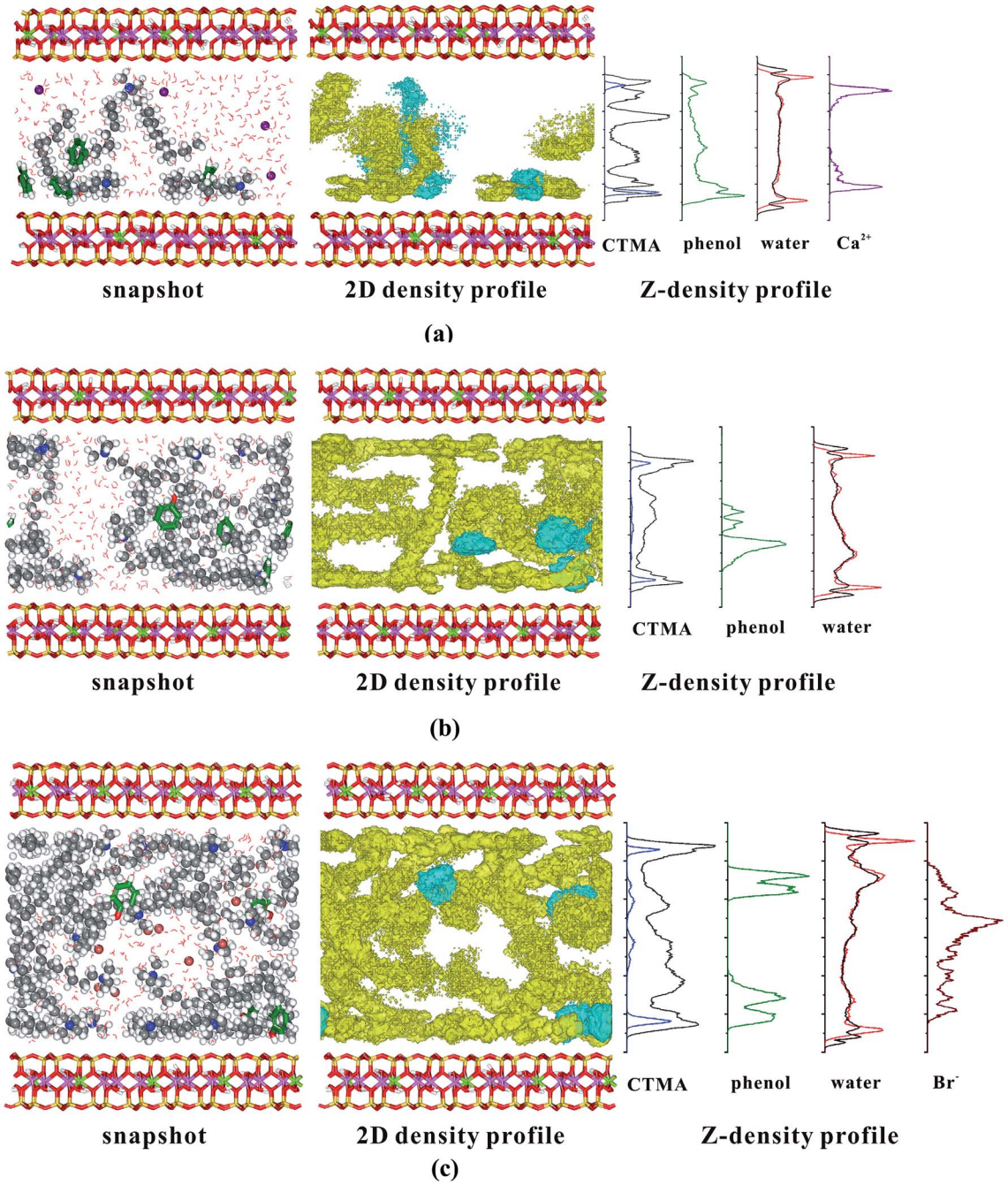


Fig. 1 Snapshots (left graph), 2D density profiles (middle graph), and *Z*-density profiles (right graph) of hydrated CTMA-Mt with different loading level: (a) 0.33 CEC; (b) 1.00 CEC; (c) 1.66 CEC. In the snapshots: gray ball, C3 (CTMA C on alkyl chains); blue ball, N3 (CTMA N); white ball, H3 (CTMA H); green stick, phenol; purple ball, Ca ion; red line, water. In the 2D density profiles: C3 in yellow; CR in blue. In the *Z*-density profiles: N3 in blue; C3 in dark gray; CR in green; OW (water O) in red; HW (water H) in black; $Ca^{2+}$ in purple; $Br^{-}$ in brown.

electrostatic repulsion between $Br^{-}$ and negatively charged siloxane surface as well. The RDF profiles of Br-HW and Br-HC (Fig. 2b) indicated that hydrated $Br^{-}$ does not directly interact with CTMA as well. However, the RDF of Br-N3 (CTMA nitrogen) reveals the bonding of hydrated $Br^{-}$ anions to the charged head group of CTMA (Fig. 2b).

Within the interlayer spaces of 1.0 CTMA-Mt and 1.66 CTMA-Mt, water molecules were shown to mostly occupy the spaces between CTMA aggregates (Fig. 1b and c). As for 0.33 CTMA-Mt, water molecules occupied a large portion of the interlayer space, and some water molecules could even penetrate into the loosely associated CTMA aggregates (Fig. 1a). On the other hand, the *Z*-density profiles showed that water molecules had high density above the siloxane surface for all the three samples, which could be attributed to the hydration of the siloxane surface and the formation of H-bonds.[26–30,43–46]

Table 1 Average H-bond numbers formed for each phenol molecule (with water molecules), the self-diffusion coefficients of C3 ($D_{C3}$) and CP ($D_{CR}$), and CTMA packing density ($d_{CTMA}$). $N_D$: H-bond numbers in the case phenol as proton donor; $N_A$: H-bond numbers in the case phenol as proton acceptor; $N_{total}$: total H-bond numbers for each phenol ($N_D$ + $N_A$)

| | Average H-bond number | | | | | | |
|---|---|---|---|---|---|---|---|
| Sample | $N_D$ | $N_A$ | $N_{total}$ | $N_D/N_A$ | $D_{C3}$ ($10^{-11}$ m$^2$ s$^{-1}$) | $D_{CR}$ ($10^{-11}$ m$^2$ s$^{-1}$) | $d_{CTMA}$ (g cm$^{-3}$) |
| 0.33 CTMA-Mt | 0.280 | 0.143 | 0.423 | 1.96 | 3.2 | 4.9 | 0.602 |
| 1.0 CTMA-Mt | 0.283 | 0.105 | 0.388 | 2.69 | 2.3 | 1.9 | 0.764 |
| 1.66 CTMA-Mt | 0.271 | 0.064 | 0.335 | 4.25 | 1.7 | 2.0 | 0.898 |

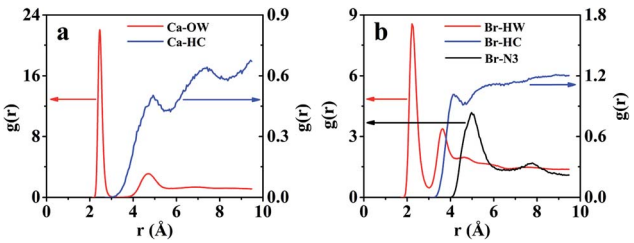


Fig. 2 RDF profiles of the hydrated CTMA-Mt. (a) Ca-OW and Ca-HC for 0.33 CTMA-Mt; (b) Br-HW, Br-HC, and Br–N3 for 1.66 CTMA-Mt.

## 2. Effects of inorganic ions on the sorption of phenol molecules

Although several experimental studies have proposed that inorganic ions affect the sorption of OCs on organoclays,[19,22] modelling studies are still lacking. Xu *et al.*[19] suggested that the hydration of the inorganic ions decreases the hydrophobicity of the interlayer spaces, leading to weaker sorption capacity of the organoclays. However, no direct structural evidences were presented, as the experimental techniques can hardly provide high resolution information of the arrangement and hydration of inorganic ions in water saturated organoclays.

Our results demonstrated that the hydrated inorganic ions ($Ca^{2+}$ and $Br^-$) were mainly located in the water solvent and generally would not be incorporated into the CTMA aggregates and the uptake of phenol is partition process. As such, one might expect the influence of the hydrated inorganic ions on the partition behaviors of the CTMA aggregates would be less than the bulk water case. However, it is worth noting that the nano-sized surfactant aggregates have large interface with the interlayer water, and it is likely that some of the OCs would be sorbed at/near this interface. In this instance, the inorganic ions affect the sorption of OCs on organoclays. As water molecules surrounding $Ca^{2+}$ showed particular orientation, *i.e.*, with OW (water oxygen) pointing towards $Ca^{2+}$ (Fig. 3a and 4a), they tend to act as H-bond donor and then will help the sorption of OCs with H-bond acceptor capability. On the other hand, water molecules surrounding $Br^-$ had reverse orientation (Fig. 3b and 4b), and then they will help the sorption of OCs with H-bond donor capability.

The –OH group on phenol molecule can be both H-bond donor and acceptor.[47] If the inorganic ions can affect the sorption of phenol on organoclays, the orientation of –OH group surrounding the inorganic ions (*i.e.*, $Ca^{2+}$ or $Br^-$) should be quite different. To address these points, we present the RDF between the phenol and the inorganic cations. The RDF profiles of Ca-OP (–OH oxygen on phenol), Ca-HP (–OH hydrogen on phenol), Br-OP, and Br-HP were compared in Fig. 3c and d and showed that Ca ions interacted more strongly with the OP while the $Br^-$ ions with the HP, consistent with our hypothesis. Interestingly, the RDFs clearly showed that phenol interacts only with the hydration shell of $Ca^{2+}$ while it interacts directly with $Br^-$. Direct interactions between OCs with inorganic ions were also reported in previous studies, particularly for the ions with relatively weak hydration capacity such as Cs and K.[48–50] The hydration enthalpy of $Br^-$ is indeed −328 kJ mol$^{-1}$, close to that of $K^+$ (−340 kJ mol$^{-1}$), but much smaller than that of $Ca^{2+}$ (−1616 kJ mol$^{-1}$).[51] It is worth noting that one may expect that when anions with stronger hydration capacity (*e.g.*, $F^-$, −504 kJ mol$^{-1}$)[51] are presented in the interlayer, phenol may interact with the hydration shell instead of the anion. This is clearly not the case in this study.

The snapshots of 0.33 CTMA-Mt and 1.66 CTMA-Mt after removing CTMA were plotted to show the interlayer H-bond network (Fig. 4). Water molecules around inorganic ions showed special orientation, *i.e.*, with OW pointing toward $Ca^{2+}$

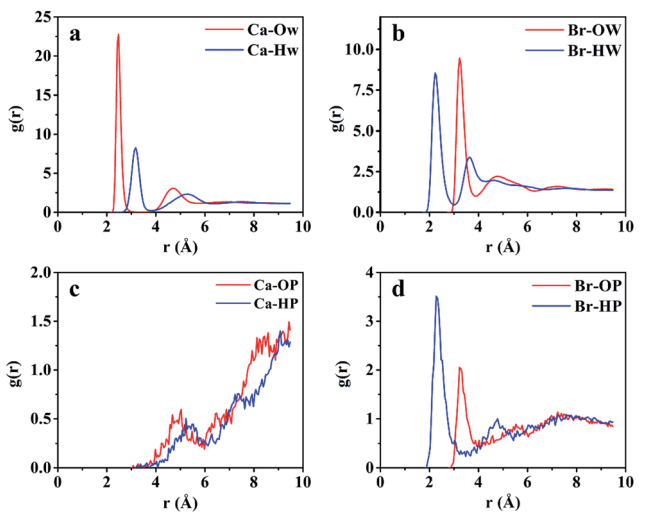


Fig. 3 RDF profiles of the hydrated CTMA-Mt. (a) Ca-OW and Ca-HW for 0.33 CTMA-Mt; (b) Br-OW and Br-HW for 1.66 CTMA-Mt; (c) Ca-OP (phenol O) and Ca-HP (phenol H) for 0.33 CTMA-Mt; (d) Br-OP and Br-HP for 1.66 CTMA-Mt.

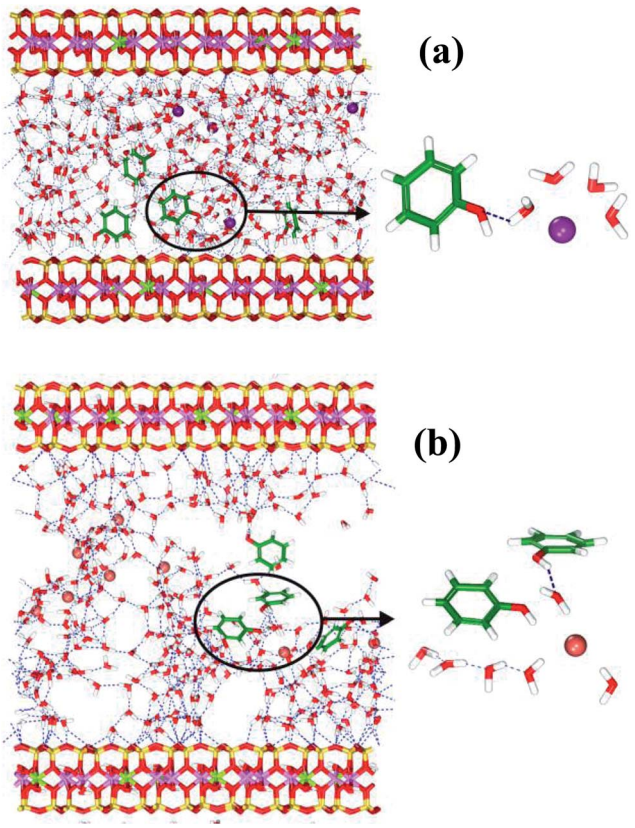


Fig. 4 H-bond network within CTMA-Mt interlayer (CTMA molecules were removed for better view). H-bond formed between water and phenol near $Ca^{2+}$ or $Br^{-}$ ions were particularly shown. (a) 0.33 CTMA-Mt; (b) 1.66 CTMA-Mt.

on 0.33 CTMA-Mt while HW pointing toward $Br^{-}$ on 1.66 CTMA-Mt. As a result, water molecules around $Ca^{2+}$ could be H-bond donor when interacting with phenol molecules (Fig. 4a), while those around $Br^{-}$ tended to be H-bond acceptor (Fig. 4b). Moreover, phenol may also penetrate the hydration shell and directly interact with $Br^{-}$.

The average numbers of H-bond formed between water molecules and each phenol molecule were calculated (Table 1). One should notice that phenol molecules on all the three samples were more likely to be H-bond donor (D) rather than acceptor (A) when forming H-bond with water molecules, which should be attributed to its physicochemical properties, *i.e.*, stronger ability to be H-bond donor than acceptor.[48] With increasing CTMA loading level, the total number of H-bonds for each phenol molecules decreased drastically, which is consistent with the phenol molecules being located within the CTMA aggregates (as the aggregates became larger). In addition, the numbers of D type H-bond did not change much with increasing CTMA loading level, while those of A type decreased drastically. As a result, the ratio of D/A increased significantly with increasing CTMA loading level, which again proved that the hydrated inorganic ions can evidently affect the formation of H-bond between phenol and water molecules. However, one should also notice that the number of H-bonds formed between water and phenol molecules on CTMA-Mt was smaller than those in bulk water (~0.78 H-bond on average according to our calculation), which is consistent with the fact that phenol molecules were mainly located in the CTMA aggregates.

## 3. Comparison with previous experimental studies

Combining the modelling results of this work with previous experimental studies provides novel insights for clarifying the sorptive characteristics of organoclays. Zhu *et al.*[52] studied the effects of surfactant loading level on the sorption thermodynamics of CTMA-Mt toward naphthalene, showing that the sorption process was primarily driven by the entropy term, while the enthalpy term showed positive contribution at low CTMA loading level (*i.e.*, ~0.2 CEC and ~1.0 CEC) and negative contribution at high loading level (~1.8 CEC). The sorption enthalpy of naphthalene was notably less exothermic than the desolvation enthalpy of naphthalene, which confirmed a partition into the CTMA aggregates rather than a condensation on the surface of CTMA-Mt, well in agreement with the modeling results of this study. Combining the characterization results and the calculated thermodynamic values, they further proposed that CTMA within the interlayer of CTMA-Mt could form various organic phases for the sorption of OCs as the loading level changed.[52] Our modelling results clearly demonstrated the CTMA aggregates change in size and packing density with increasing CTMA loading level, not only consistent with their proposal, but also reveals the microstructure of CTMA aggregates at atomic level.

Recently, Zhu *et al.*[52] studied the effect of CTMA loading level (0.4 CEC, 1.0 CEC, and 1.6 CEC) on the sorptive characteristics of CTMA-Mt using polyparameter linear free energy relationships (pp-LFERs) analysis, which directly show the relative contributions of individual intermolecular interactions to a sorption process.[53–56] Their results demonstrated that the driving forces for the sorption of OCs in CTMA-Mt arise from weaker cohesive characteristics, stronger dispersion interaction and H-bond acceptor capacity, compared to bulk water. On the other hand, CTMA-Mt showed weaker polar/polarization interaction and H-bond donor capacity, which had a negative contribution to the sorption process. These results suggested that the OCs should be primarily sorbed into organic phases (*i.e.*, CTMA aggregates), consistent with the modelling results of this work as well. The strong H-bond acceptor capacity was suggested to rise from the oxygen atoms on the siloxane surfaces, which could accept hydrogen atoms to form H-bond in our modelling results.

With increasing CTMA loading level, they further showed that the CTMA-Mt became more cohesive with stronger polarization interaction and H-bond acceptor capacity, but weaker H-bond donor capacity, also shown in our modelling results. As the size of CTMA aggregates became larger, OCs were more likely to be sorbed within the aggregates rather than at their surface, which then caused stronger dispersion interaction between CTMA-Mt and OCs. As is well known, OCs generally have stronger dispersion interaction with organic phases than with water molecules (*i.e.*, easier to form a cavity for the accommodation of OCs molecule).[30,53,54] More cohesive

characteristics of CTMA-Mt with higher CTMA loading should be caused by the larger packing density of CTMA aggregates, as in this case creating a cavity within the aggregates should consume more free energy. As the interlayer inorganic ions changed from cations to anions, the interlayer water molecules then behaved more likely as H-bond donor than acceptor, which then weakened the H-bond donor capacity of the resulting CTMA-Mt. As such, our modelling results correlated with previous pp-LFERs studies well, and gave atom-level insight to explain the macroscopic sorption property (*i.e.* uptake of OCs) of CTMA-Mt depending on the CTMA loading level.

## Conclusions

In summary, molecular modelling gave atom-level insight into the interlayer structure of CTMA-Mt by showing the arrangement of interlayer species. Our results provided additional information supporting that the sorption of OCs on organoclays is a partition controlled process, and OCs molecules are mainly sorbed into surfactant aggregates (*i.e.*, organic phases). Our results clearly demonstrated that the loading level of surfactant significantly affect the structure of the aggregates (*e.g.*, size, packing density, *etc.*), and accordingly their sorption affinity towards OCs. In addition, siloxane surface and interlayer inorganic ions have specific interactions with OCs, particularly those containing H-bond acceptor/donor capabilities, which then can have additional effects to the sorption behaviors of organoclays.

## Acknowledgements

This work was financially supported by the "One Hundred Talents program" of the Chinese Academy of Sciences (KZZD-EW-TZ-10), grants from the National Natural Science Foundation of China (41322014, 21177104), the Royal Society BP Amoco Research Fellowship (RC-H1054), and CAS/SAFEA International Partnership Program for Creative Research Teams (20140491534). Dr Molinari and Prof. Parker would like to acknowledge the EPSRC for funding (EP/I03601X/1) and the Materials Chemistry Consortium funded by EPSRC (EP/L000202) for access to the ARCHER facility. This is contribution (IS-2077) from GIGCAS.

## References

1 Y. Park, G. A. Ayoko and R. L. Frost, Application of organoclays for the adsorption of recalcitrant organic molecules from aqueous media, *J. Colloid Interface Sci.*, 2011, **354**(1), 292–305.

2 I. Fatimah and T. Huda, Preparation of cetyltrimethylammonium intercalated Indonesian montmorillonite for adsorption of toluene, *Appl. Clay Sci.*, 2013, **74**, 115–120.

3 S. A. Boyd, M. M. Mortland and C. T. Chiou, Sorption characteristics of organic-compounds on hexadecyltrimethylammonium-smectite, *Soil Sci. Soc. Am. J.*, 1988, **52**(3), 652–657.

4 S. A. Boyd, S. Shaobai, J. F. Lee and M. M. Mortland, Pentachlorophenol sorption by organo-clays, *Clays Clay Miner.*, 1988, **36**(2), 125–130.

5 J. A. Smith, P. R. Jaffe and C. T. Chiou, Effect of 10 quaternary ammonium cations on tetrachloromethane sorption to clay from water, *Environ. Sci. Technol.*, 1990, **24**(8), 1167–1172.

6 J. A. Smith and A. Galan, Sorption of nonionic organic contaminants to single and dual organic cation bentonites from water, *Environ. Sci. Technol.*, 1995, **29**(3), 685–692.

7 L. Zhu, Y. Li and J. Zhang, Sorption of organobentonites to some organic pollutants in water, *Environ. Sci. Technol.*, 1997, **31**(5), 1407–1410.

8 G. D. Yuan, B. K. G. Theng, G. J. Churchman and W. P. Gates, Clays and clay minerals for pollution control, in *Handbook of Clay Science*, ed. F. Bergaya and G. Lagaly, Elsevier, Amsterdam, 2nd edn, 2013, pp. 587–644.

9 P. G. Slade and W. P. Gates, The swelling of HDTMA smectites as influenced by their preparation and layer charges, *Appl. Clay Sci.*, 2004, **25**(1–2), 93–101.

10 W. F. Jaynes and S. A. Boyd, Clay mineral type and organic-compound sorption by hexadecyltrimethlyammonium-exchanged clays, *Soil Sci. Soc. Am. J.*, 1991, **55**(1), 43–48.

11 G. Y. Sheng, S. H. Xu and S. A. Boyd, Mechanism(s) controlling sorption of neutral organic contaminants by surfactant-derived and natural organic matter, *Environ. Sci. Technol.*, 1996, **30**(5), 1553–1557.

12 Y. H. Shen, Phenol sorption by organoclays having different charge characteristics, *Colloids Surf., A*, 2004, **232**(2–3), 143–149.

13 R. Zhu, L. Zhu and L. Xu, Sorption characteristics of CTMA–bentonite complexes as controlled by surfactant packing density, *Colloids Surf., A*, 2007, **294**(1–3), 221–227.

14 R. Zhu, L. Zhu, J. Zhu and L. Xu, Structure of surfactant–clay complexes and their sorptive characteristics toward HOCs, *Sep. Purif. Technol.*, 2008, **63**(1), 156–162.

15 L. Zhu, B. Chen, S. Tao and C. T. Chiou, Interactions of organic contaminants with mineral-adsorbed surfactants, *Environ. Sci. Technol.*, 2003, **37**(17), 4001–4006.

16 B. L. Chen, L. Z. Zhu and J. X. Zhu, Configurations of the bentonite-sorbed myristylpyridinium cation and their influences on the uptake of organic compounds, *Environ. Sci. Technol.*, 2005, **39**(16), 6093–6100.

17 J. Zhu, L. Zhu, R. Zhu and B. Chen, Microstructure of organobentonites in water and the effect of steric hindrance on the uptake of organic compounds, *Clays Clay Miner.*, 2008, **56**(2), 144–154.

18 S. L. Bartelt-Hunt, S. E. Burns and J. A. Smith, Nonionic organic solute sorption onto two organobentonites as a function of organic-carbon content, *J. Colloid Interface Sci.*, 2003, **266**(2), 251–258.

19 L. Xu and L. Zhu, Structures of OTMA- and DODMA-bentonite and their sorption characteristics towards organic compounds, *J. Colloid Interface Sci.*, 2009, **331**(1), 8–14.

20 L. Xu, M. Zhang and L. Zhu, Adsorption–desorption behavior of naphthalene onto CDMBA modified bentonite:

 

contribution of the pi–pi interaction, *Appl. Clay Sci.*, 2014, **100**, 29–34.
21 V. N. Nguyen, T. D. C. Nguyen, T. P. Dao, H. T. Tran, D. B. Nguyen and D. H. Ahn, Synthesis of organoclays and their application for the adsorption of phenolic compounds from aqueous solution, *J. Ind. Eng. Chem.*, 2013, **19**(2), 640–644.
22 J. L. Bonczek, W. G. Harris and P. Nkedi-Kizza, Monolayer to bilayer transitional arrangements of hexadecyltrimethylammonium cations on Na-montmorillonite, *Clays Clay Miner.*, 2002, **50**(1), 11–17.
23 J. A. Greathouse and R. T. Cygan, Water structure and aqueous uranyl(VI) adsorption equilibria onto external surfaces of beidellite, montmorillonite, and pyrophyllite: results from molecular simulations, *Environ. Sci. Technol.*, 2006, **40**(12), 3865–3871.
24 R. T. Cygan, J. A. Greathouse, H. Heinz and A. G. Kalinichev, Molecular models and simulations of layered materials, *J. Mater. Chem.*, 2009, **19**(17), 2470–2481.
25 J. A. Greathouse and R. T. Cygan, Molecular simulation of clay minerals, in *Handbook of Clay Science*, ed. F. Bergaya and G. Lagaly, 2nd edn, Elsevier, Amsterdam, 2013, pp. 405–424.
26 C. P. Morrow, A. O. Yazaydin, M. Krishnan, G. M. Bowers, A. G. Kalinichev and R. J. Kirkpatrick, Structure, Energetics, and Dynamics of Smectite Clay Interlayer Hydration: Molecular Dynamics and Metadynamics Investigation of Na-Hectorite, *J. Phys. Chem. C*, 2013, **117**(10), 5172–5187.
27 L. Zhang, X. Lu, X. Liu, J. Zhou and H. Zhou, Hydration and Mobility of Interlayer Ions of (Nax, Cay)-Montmorillonite: A Molecular Dynamics Study, *J. Phys. Chem. C*, 2014, **118**(51), 29811–29821.
28 Q. Zhou, W. Shen, J. Zhu, R. Zhu, H. He, J. Zhou and P. Yuan, Structure and dynamic properties of water saturated CTMA-montmorillonite: molecular dynamics simulations, *Appl. Clay Sci.*, 2014, **97–98**, 62–71.
29 J. Zhou, X. Lu, J. Zhu, X. Liu, J. Wei, Q. Zhou, P. Yuan and H. He, Interlayer structure and dynamics of HDTMA(+)-intercalated rectorite with and without water: a molecular dynamics study, *J. Phys. Chem. C*, 2012, **116**(24), 13071–13078.
30 R. Zhu, W. Chen, T. V. Shapley, M. Molinari, F. Ge and S. C. Parker, Sorptive characteristics of organomontmorillonite toward organic compounds: a combined LFERs and molecular dynamics simulation study, *Environ. Sci. Technol.*, 2011, **45**(15), 6504–6510.
31 R. Zhu, W. Hu, Z. You, F. Ge and K. Tian, Molecular dynamics simulation of TCDD adsorption on organo-montmorillonite, *J. Colloid Interface Sci.*, 2012, **377**, 328–333.
32 Q. Zhao and S. E. Burns, Molecular dynamics simulation of secondary sorption behavior of montmorillonite modified by single chain quaternary ammonium cations, *Environ. Sci. Technol.*, 2012, **46**(7), 3999–4007.
33 Q. Zhao and S. E. Burns, Modeling sorption and diffusion of organic sorbate in hexadecyltrimethylammonium-modified clay nanopores – a molecular dynamics simulation study, *Environ. Sci. Technol.*, 2013, **47**(6), 2769–2776.
34 T. V. Shapley, M. Molinari, R. Zhu and S. C. Parker, Atomistic modeling of the sorption free energy of dioxins at clay–water interfaces, *J. Phys. Chem. C*, 2013, **117**(47), 24975–24984.
35 W. Loewenstein, The distribution of aluminum in the tetrahedra of silicates and aluminates, *Am. Mineral.*, 1954, **39**(1–2), 92–96.
36 W. Smith and T. Forester, DL_POLY_2. 0: a general-purpose parallel molecular dynamics simulation package, *J. Mol. Graphics*, 1996, **14**(3), 136–141.
37 R. T. Cygan, J. J. Liang and A. G. Kalinichev, Molecular models of hydroxide, oxyhydroxide, and clay phases and the development of a general force field, *J. Phys. Chem. B*, 2004, **108**(4), 1255–1266.
38 H. Berendsen, J. Postma, W. van Gunsteren and J. Hermans, Interaction models for water in relation to protein hydration, in *Intermolecular Forces*, ed. B. Pullman, Reidel, Dordrecht, 1981, pp. 331–342.
39 P. Dauberosguthorpe, V. A. Roberts, D. J. Osguthorpe, J. Wolff, M. Genest and A. T. Hagler, Structure and energetics of ligand-binding to proteins – *Escherichia coli* dihydrofolate reductase trimethoprim, a drug-receptor system, *Proteins: Struct., Funct., Genet.*, 1988, **4**(1), 31–47.
40 J. C. Crabtree, M. Molinari, S. C. Parker and J. A. Purton, Simulation of the Adsorption and Transport of $CO_2$ on Faujasite Surfaces, *J. Phys. Chem. C*, 2013, **117**(42), 21778–21787.
41 D. M. S. Martins, M. Molinari, M. A. Goncalves, J. P. Mirao and S. C. Parker, Toward Modeling Clay Mineral Nanoparticles: The Edge Surfaces of Pyrophyllite and Their Interaction with Water, *J. Phys. Chem. C*, 2014, **118**(47), 27308–27317.
42 E. Guardia, J. Marti, L. Garcia-Tarres and D. Laria, A molecular dynamics simulation study of hydrogen bonding in aqueous ionic solutions, *J. Mol. Liq.*, 2005, **117**(1–3), 63–67.
43 J. Wang, A. G. Kalinichev and R. J. Kirkpatrick, Effects of substrate structure and composition on the structure, dynamics, and energetics of water at mineral surfaces: a molecular dynamics modeling study, *Geochim. Cosmochim. Acta*, 2006, **70**(3), 562–582.
44 J. Wang, A. G. Kalinichev, R. J. Kirkpatrick and R. T. Cygan, Structure, energetics, and dynamics of water adsorbed on the muscovite (001) surface: a molecular dynamics simulation, *J. Phys. Chem. B*, 2005, **109**(33), 15893–15905.
45 W. B. F. Ngouana and A. G. Kalinichev, Structural arrangements of isomorphic substitutions in smectites: molecular simulation of the swelling properties, inter layer structure, and dynamics of hydrated cs-montmorillonite revisited with new clay models, *J. Phys. Chem. C*, 2014, **118**(24), 12758–12773.
46 V. Marry, B. Rotenberg and P. Turq, Structure and dynamics of water at a clay surface from molecular dynamics simulation, *Phys. Chem. Chem. Phys.*, 2008, **10**(32), 4802–4813.

47 M. H. Abraham, H. S. Chadha, A. R. E. Leitao, R. C. Mitchell, W. J. Lambert, R. Kaliszan, A. Nasal and P. Haber, Determination of solute lipophilicity, as log P(octanol) and log P(alkane) using poly(styrene-divinylbenzene) and immobilised artificial membrane stationary phases in reversed-phase high-performance liquid chromatography, *J. Chromatogr. A*, 1997, **766**(1–2), 35–47.

48 X. Liu, R. Zhu, J. Ma, F. Ge, Y. Xu and Y. Liu, Molecular dynamics simulation study of benzene adsorption to montmorillonite: influence of the hydration status, *Colloids Surf., A*, 2013, **434**, 200–206.

49 V. Aggarwal, H. Li, S. A. Boyd and B. J. Teppen, Enhanced sorption of trichloroethene by smectite clay exchanged with $Cs^{+}$, *Environ. Sci. Technol.*, 2006, **40**(3), 894–899

50 M. A. Chappell, D. A. Laird, M. L. Thompson, H. Li, B. J. Teppen, V. Aggarwal, C. T. Johnston and S. A. Boyd, Influence of smectite hydration and swelling on atrazine sorption behavior, *Environ. Sci. Technol.*, 2005, **39**(9), 3150–3156.

51 J. Barrett, *Inorganic Chemistry in Aqueous Solution*, Royal Society of Chemistry, Cambridge, 2003.

52 R. Zhu and L. Zhu, Thermodynamics of naphthalene sorption to organoclays: role of surfactant packing density, *J. Colloid Interface Sci.*, 2008, **322**(1), 27–32.

53 R. Zhu, W. Chen, Y. Liu, J. Zhu, F. Ge and H. He, Application of linear free energy relationships to characterizing the sorptive characteristics of organic contaminants on organoclays from water, *J. Hazard. Mater.*, 2012, **233**, 228–234.

54 S. Endo and K.-U. Goss, Applications of Polyparameter Linear Free Energy Relationships in Environmental Chemistry, *Environ. Sci. Technol.*, 2014, **48**(21), 12477–12491.

55 T. H. Nguyen, K. U. Goss and W. P. Ball, Polyparameter linear free energy relationships for estimating the equilibrium partition of organic compounds between water and the natural organic matter in soils and sediments, *Environ. Sci. Technol.*, 2005, **39**(4), 913–924.

56 M. Vitha and P. W. Carr, The chemical interpretation and practice of linear solvation energy relationships in chromatography, *J. Chromatogr. A*, 2006, **1126**(1–2), 143–194.